Synthesis, Characterization, and Dynamic Behavior of $Os_2Pt(CO)_8(PPh_3)_2$: A Trinuclear Osmium−Platinum Cluster with Flexible Metal Framework

Jason Cooke,† R. E. D. McClung, and Josef Takats*

Department of Chemistry, University of Alberta, Edmonton, Alberta, Canada T6G 2G2

Robin D. Rogers

Department of Chemistry, Northern Illinois University, DeKalb, Illinois 60115

Received December 5, 1995⊗

Reaction of $Os_2(CO)_8(\mu\text{-}\eta^1,\eta^1\text{-}C_2H_4)$ with $(\eta^2\text{-}C_2H_4)Pt(PPh_3)_2$ gives predominantly the heterotrinuclear cluster $Os_2Pt(CO)_8(PPh_3)_2$, **1**. The reaction is accompanied by redistribution of the PPh_3 ligand, and as a result, compound **1** exists in solution as three isomers (**1a**−**c**) due to the presence and disposition of a phosphine ligand on both Os and Pt. The nature of the isomers was deduced from a combination of ^{13}C, ^{31}P, and ^{195}Pt NMR spectroscopies, and the solid-state structure of the major isomer was corroborated by a single-crystal X-ray analysis. The isomers interconvert on the NMR time scale, and the mechanisms and energetics of the isomerization processes were determined by ^{31}P NMR selective inversion magnetization transfer experiments. Two pathways for isomer exchange were identified. Isomers **1a** and **1b** exchange *via* an "olefin type" rotation of the diosmium fragment about the platinum center, whereas interconversion between **1a** and **1c** is accomplished by a restricted trigonal twist at the phosphine-substituted osmium center; the energetics for the processes are $\Delta H^{\ddagger} = 10.1(2)$ kcal·mol^{-1}, $\Delta S^{\ddagger} = -13.1(11)$ eu and $\Delta H^{\ddagger} = 10.7(3)$ kcal·mol^{-1}, $\Delta S^{\ddagger} = -5.2(12)$ eu, respectively. The mechanism of the **1a** ⇄ **1c** exchange was confirmed by ^{13}C NMR spin saturation transfer experiments.

Introduction

Recent interest in heteronuclear cluster compounds of platinum,[1] in particular those in combination with group eight metals (Fe, Ru, Os),[2] is the direct result of the recognized connection between such clusters and bimetallic alloy catalysts.[3] Despite the wealth of ongoing research, the simple trinuclear carbonyl clusters of iron or ruthenium and platinum are as yet unknown. In the case of iron, the related phosphine-substituted trinuclear compounds $Fe_2Pt(CO)_9L$ and $Fe_2Pt(CO)_8L_2$ (L = PR_3, L_2 = $Ph_2PCH_2CH_2PPh_2$ (dppe)),[4] and the cycloocta-1,5-diene adduct $Fe_2Pt(CO)_8(COD)$,[5] have been reported (Chart 1). For ruthenium, clusters of the type $Ru_2Pt(CO)_7(PR_3)_3$ and $RuPt_2(CO)_5(PR_3)_3$ are known,[6] but to date, the only species bearing structural similarity to the iron−platinum clusters is $Ru_2Pt(CO)_8(dppe)$, obtained by phosphine-induced cleavage of the hexanuclear Pt−Ru cluster (eq 1)[2b] or as one of two products from the reaction of $Ru_3(CO)_{12}$ with $Pt(dppe)_2$.[6] In the case of osmium, the parent decacarbonyl $Os_2Pt(CO)_{10}$ has been characterized,[7] but owing to its thermal instability and ready dimerization to $Os_4Pt_2(CO)_{18}$ (eq

Chart 1

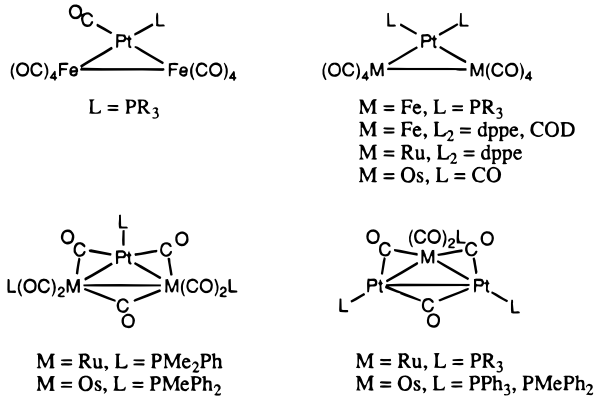

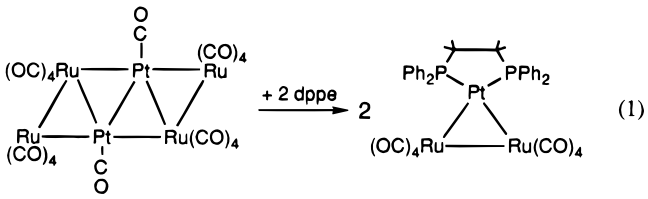

(1)

† NSERC Undergraduate Research Awardee.

⊗ Abstract published in *Advance ACS Abstracts,* August 15, 1996.

(1) Farrugia, L. J. *Adv. Organomet. Chem.* **1990**, *31*, 301.

(2) For example, see: (a) Adams, R. D.; Arafa, I.; Chen, G.; Lii, J.; Wang, J. *Organometallics* **1990**, *9*, 2350 (M = Fe). (b) Adams, R. D.; Chen, G.; Wang, J.; Wu, W. *Organometallics* **1990**, *9*, 1339 (M = Ru). (c) Adams, R. D.; Chen, G.; Lii, J.; Wu, W. *Inorg. Chem.* **1991**, *30*, 1007 (M = Os).

(3) *The Chemistry of Heteronuclear Clusters and Multimetallic Catalysts*; Proceedings of the Seminar Held at Albertus Magnus College, Königstein, FRG, Sept 7−11, 1987; Adams, R. D., Herrmann, W. A., Eds. *Polyhedron* **1988**, *7*, 2251−2462.

(4) (a) Bruce, M. I.; Shaw, G.; Stone, F. G. A. *J. Chem. Soc., Dalton Trans.* **1972**, 1082. (b) Mason, R.; Zubieta, J. *J. Chem. Soc., Chem. Commun.* **1972**, 200.

(5) Farrugia, L. J.; Howard, J. A. K.; Mitrprachachon, P.; Stone, F. G. A.; Woodward, P. *J. Chem. Soc., Dalton Trans.* **1981**, 1134.

(6) Bruce, M. I.; Shaw, G.; Stone, F. G. A. *J. Chem. Soc., Dalton Trans.* **1972**, 1781.

(7) Sundberg, P. *J. Chem. Soc., Chem. Commun.* **1987**, 1307.

S0276-7333(95)00938-1 CCC: $12.00

2), only recently has a high-quality X-ray crystal structure determination on the complex been obtained.[2c]

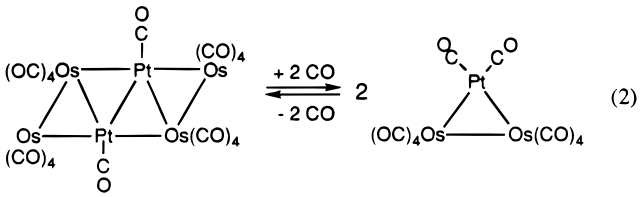

(2)

A prevalent difficulty in targeted cluster synthesis is the occasional lack of simple building blocks from which to generate more complex structures in a rational manner. Notable exceptions are the metal−carbyne synthon ($L_nM{\equiv}CR$), pioneered by Stone and his coworkers,[8] and the bridging ligand promoted agglomerization of metal-containing fragments.[9] In the present context, Stone and co-workers had some success in the preparation of $Fe_2Pt(CO)_8L_2$ complexes by reacting $Fe_2(CO)_9$ with 1 equiv of PtL_4 but were hampered by low yields and formation of mononuclear $Fe(CO)_4L$ and $Fe(CO)_3L_2$ byproducts.[4a] The only convenient syntheses of $Os_2Pt(CO)_{10}$ involve cleavage of either the hexanuclear cluster $Os_4Pt_2(CO)_{18}$ under 50 atm of CO pressure[7] or the pentanuclear cluster $Os_3Pt_2(CO)_{10}(COD)_2$ by CO purge at 25 °C.[2c]

Bimetallic osmium carbonyl complexes, which could act as suitable precursors for the generation of higher nuclearity clusters, became available with the facile photochemical synthesis of diosmacyclobutane, $Os_2(CO)_8(\mu\text{-}\eta^1,\eta^1\text{-}C_2H_4)$,[10] and the related, but more labile, propylene analogue.[11] Although the ready loss of ethylene from $Os_2(CO)_8(\mu\text{-}\eta^1,\eta^1\text{-}C_2H_4)$ was initially believed to proceed *via* a concerted cycloreversion,[12a] recent synthetic[13] and kinetic[14] studies by Norton have demonstrated that the fragmentation of diosmacyclobutane does not involve direct generation of $(OC)_4Os{=}Os(CO)_4$ but proceeds rather by an intermediate in which the bridging olefin has slipped to η^2 coordination at one osmium center. This latter point of view is in accord with matrix isolation[11,15] and solution flash photolysis[15] studies on these diosmacycles. Whatever the mechanistic intricacies, the feature of synthetic import is that these diosmacyclobutanes generally act as sources of the unsaturated $Os_2(CO)_8$ fragment. This has been demonstrated in olefin[12] and alkyne[10b] exchange reactions and, following Stone's insightful application of the isolobal analogy[16] to the rational synthesis of trimetallacyclopropanes,[17] in the preparation of the heterotrimetallic complexes $Os_2Rh(CO)_9(\eta^5\text{-}C_5R_5)$ (R = H, Me).[18] A recent extension of this methodology to the reaction of $Os_2(CO)_8(\mu\text{-}\eta^1,\eta^1\text{-}C_2H_4)$ with $(\eta^5\text{-}C_5H_5)Rh(CO)PR'_3$ (R′ = Me, Ph) introduced complications arising from redistribution of the phosphine ligand from rhodium to an osmium center.[19]

With these established precedents, it was of interest to investigate the reaction of octacarbonyldiosmacyclobutane with an unsaturated platinum fragment. The greater stability of phosphine-substituted platinum complexes[7] and the convenient synthesis of $(\eta^2\text{-}C_2H_4)Pt(PPh_3)_2$[20] made this the reagent of choice for such a study. Previously, Beringhelli and co-workers successfully reacted $(\eta^2\text{-}C_2H_4)Pt(PPh_3)_2$ with the formally unsaturated bimetallic complex $Re_2(\mu\text{-}H)_2(CO)_8$ and obtained $Re_2Pt(\mu\text{-}H)_2(CO)_8(PPh_3)_2$.[21]

Results and Discussion

Synthesis and Characterization. As indicated in the introduction, octacarbonyldiosmacyclobutane is a useful synthetic source of the reactive $Os_2(CO)_8$ fragment. While previous cases[10b,12,18,19] required either mild heating or photolysis to initiate reaction, $(\eta^2\text{-}C_2H_4)Pt(PPh_3)_2$ reacts readily at ambient temperature to form predominantly an orange complex in good yield (eq 3).

$$\begin{matrix}Os_2(CO)_8(\mu\text{-}\eta^1,\eta^1\text{-}C_2H_4)\\ +\\ (\eta^2\text{-}C_2H_4)Pt(PPh_3)_2\end{matrix} \xrightarrow{\text{benzene}} \begin{matrix}Os_2Pt(CO)_8(PPh_3)_2\\ \textbf{(1)}\ (73\%)\end{matrix} \quad (3)$$

The mass spectrum shows the molecular ion, followed by the loss of eight carbonyl groups. The product is isolated by chromatography and is thermally stable, in contrast to the parent $Os_2Pt(CO)_{10}$ complex which, in the absence of a CO atmosphere, readily dimerizes to form $Os_4Pt_2(CO)_{18}$ (eq 1).[7] Clearly, the presence of the two phosphine ligands in **1** stabilizes the trinuclear cluster and disfavors ligand loss which would lead to the formation of clusters of higher nuclearity. A similar example of this type of stabilization by a phosphine ligand is the dppe-induced cleavage of $Ru_4Pt_2(CO)_{18}$ (eq 1).[2b]

The infrared spectrum of the product in pentane shows 10 terminal carbonyl stretching bands; their number and complexity indicate the presence of isomers and hints at an asymmetric cluster. For instance, symmetric complexes of the type $Fe_2Pt(CO)_8L_2$ (L = PR_3) show only five or six terminal carbonyl stretching bands in hydrocarbon solvents.[4a] The presence of isomers was also established in $Re_2Pt(\mu\text{-}H)_2(CO)_8(PPh_3)_2$.[21]

The NMR spectra are temperature dependent. The ambient-temperature ^{31}P NMR spectrum, Figure 1, shows two well-separated resonances; the downfield signal is quite broad. Cooling the sample to −70 °C reveals a mixture of three distinct isomers in a 4.7:3.4:1.0 (**1a**:**1b**:**1c**) ratio. Each isomer has two phosphine ligands with clearly dissimilar chemical environments. The downfield signal in each case (P_a, P_c, P_e) has platinum satellites separated by *ca.* 3000 Hz and is thus

(8) Stone, F. G. A. *Pure Appl. Chem.* **1986**, *58*, 529.
(9) (a) Adams, R. D. *Polyhedron* **1985**, *83*, 203. (b) Adams, R. D. *Coord. Chem. Rev.* **1985**, *65*, 219. (c) Shaw, B. L.; Smith, M. J.; Stretton, G. N.; Thornton-Pett, M. *J. Chem. Soc., Dalton Trans.* **1988**, 2099 and references therein. (d) Braunstein, P.; Knorr, M.; Stährfeldt, T. *J. Chem. Soc., Chem. Commun.* **1994**, 1913 and references therein.
(10) (a) Burke, M. R.; Takats, J.; Grevels, F. W.; Reuvers, J. G. A. *J. Am. Chem. Soc.* **1983**, *105*, 4092. (b) Burke, M. R.; Seils, F.; Takats, J. *Organometallics* **1994**, *13*, 1445.
(11) Haynes, A.; Poliakoff, M.; Turner, J. T.; Bender, B. R.; Norton, J. R. *J. Organomet. Chem.* **1990**, *383*, 497.
(12) (a) Hembre, R. T.; Scott, C. P.; Norton, J. R. *J. Am. Chem. Soc.* **1987**, *109*, 3468. (b) Hembre, R. T.; Ramage, D. L.; Scott, C. P.; Norton, J. R. *Organometallics* **1994**, *13*, 2995.
(13) Spetseris, N.; Norton, J. R.; Rithner, C. D. *Organometallics* **1995**, *14*, 603.
(14) Norton, J. R. Personal communication.
(15) Grevels, F. W.; Klotzbücher, W. E.; Seils, F.; Schaffner, K.; Takats, J. *J. Am. Chem. Soc.* **1990**, *112*, 1995.
(16) Hoffman, R. *Angew. Chem., Int. Ed. Engl.* **1982**, *21*, 711.
(17) Stone, F. G. A. *Angew. Chem., Int. Ed. Engl.* **1984**, *23*, 89.
(18) Washington, J.; Takats, J. *Organometallics* **1990**, *9*, 925.
(19) Cooke, J.; Takats, J. *Organometallics* **1995**, *14*, 698.
(20) Cook, C. D.; Jauhal, G. S. *J. Am. Chem. Soc.* **1968**, *90*, 1464.
(21) Beringhelli, T.; Ceriotti, A.; D'Alfonso, G.; Della Pergola, R.; Ciani, G.; Moret, M.; Sironi, A. *Organometallics* **1990**, *9*, 1053.

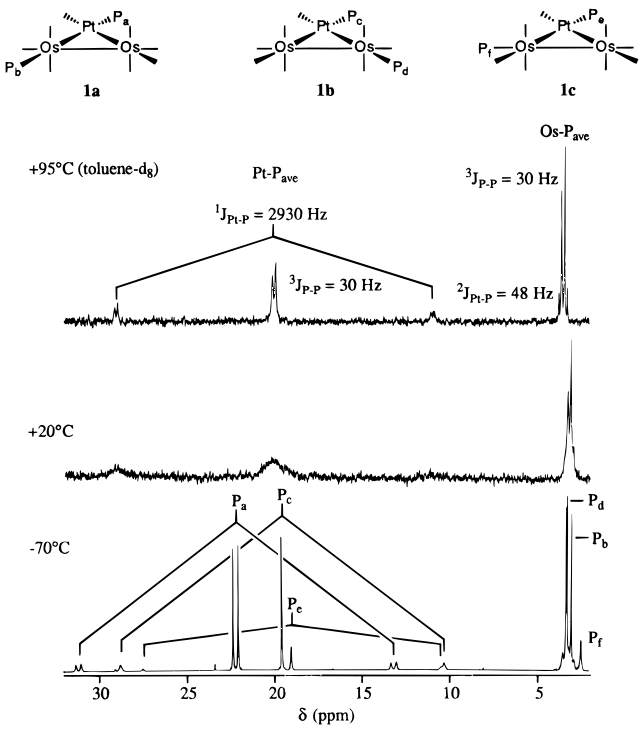

Figure 1. Variable-temperature ^{31}P NMR spectra of **1** at 162 MHz in CD_2Cl_2. Coupling data at −70 °C are as follows: **1a** ($^1J_{Pt-P_a}$ = 2913 Hz; $^2J_{Pt-P_b}$ = 60 Hz; $^3J_{P_a-P_b}$ = 49 Hz); **1b** ($^1J_{Pt-P_c}$ = 2990 Hz; $^2J_{Pt-P_d}$ = 85 Hz; $^3J_{P_c-P_d}$ = 2 Hz); **1c** ($^1J_{Pt-P_e}$ = 2756 Hz; $^2J_{Pt-P_f}$ = 25 Hz; $^3J_{P_e-P_f}$ = 5 Hz).

due to a platinum-bonded phosphorus.[22,23] The overlapping upfield signals (P_b, P_d, P_f) are flanked by platinum satellites with much smaller $^{195}Pt-^{31}P$ coupling constants and are accordingly assigned to osmium-bonded PPh_3 ligands. At +95 °C, the spectrum shows only two averaged signals; the observed platinum−phosphorus and phosphorus−phosphorus couplings are in reasonable agreement with the calculated average values. The maintenance of these couplings over the full range of temperatures and the reversible nature of the line shape changes indicate that the exchange processes averaging the P_a, P_c, and P_e signals, and the P_b, P_d, and P_f resonances, are intramolecular. Full disclosure of the rearrangement processes responsible for this is deferred for later discussion.

With the presence of a PPh_3 ligand on both Pt and Os centers having been established, and with the previous structural precedents shown in Chart 1, the presence of isomers must be due to the different dispositions of the phosphine ligand on the osmium atoms. The relative orientation of the phosphine ligands in each isomer is determined from the magnitude of the phosphorus−phosphorus and two-bond platinum−phosphorus coupling constants (refer to Figure 1). The major isomer, **1a**, exhibits a large $^3J_{P-P}$ coupling of 49 Hz and is thus the isomer in which the phosphines are along the extension of the Os−Pt bond, *trans* to one another. A two-bond phosphorus−platinum coupling of 60 Hz is also observed for the osmium-bonded PPh_3, P_b, which is consistent with the proposed *trans* relationship between P_b and Pt. Isomer **1b** displays a very small phosphorus−phosphorus coupling of 2 Hz but a large $^2J_{Pt-P}$ coupling of 85 Hz for P_d, indicating that the osmium-bonded phosphine is on the extension of the Pt−Os bond, *trans* to platinum but not *trans* to the other phosphine (P_c). In the structurally related minor isomer of $Re_2Pt(\mu\text{-}H)_2(CO)_8(PPh_3)_2$, the corresponding value of $^2J_{Pt-P}$ is 130 Hz and there is no observable phosphorus−phosphorus coupling.[21] The upfield signal of isomer **1c** shows a much smaller two-bond platinum−phosphorus coupling of 25 Hz. The decrease in the magnitude of the $^2J_{Pt-P}$ coupling constant indicates a departure from the roughly linear disposition of the phosphorus, osmium, and platinum centers found in the other two isomers;[22] P_f is thus assigned a position on the Os−Os bond extension. The observed 5 Hz phosphorus−phosphorus coupling negates the possibility of P_f being *syn* to P_e and suggests the geometry indicated in Figure 1. Steric congestion between the bulky PPh_3 ligands apparently disfavors generation of the *syn*-isomer.[24]

Low-temperature ^{195}Pt NMR spectroscopy (Figure 2) provides further structural evidence. Figure 2a shows the spectrum obtained with a sample containing natural abundance ^{13}CO ligands. The observation of three doublets is in accord with the presence of one platinum-bonded phosphine ligand in each isomer; the $^1J_{Pt-P}$ coupling constants match those observed in the −70 °C ^{31}P NMR spectrum. The **1a** and **1b** resonances are further split by the expected $^2J_{Pt-P}$ values, 60 Hz for **1a** and 75 Hz for **1b**. In **1c**, the $^2J_{Pt-P}$ coupling of 25 Hz is less than the natural ^{195}Pt line width (*ca.* 50 Hz) and the anticipated splitting is not resolved. More interesting, though, is the −70 °C ^{195}Pt NMR spectrum of a sample enriched greater than 50% in ^{13}CO. Each ^{195}Pt resonance is now flanked by ^{13}C satellites with $^1J_{Pt-C}$ of 1530, 1490, and 1520 Hz, respectively, for **1a**−**c**. The coupling constants are of the correct magntitude for carbonyl ligands which are terminally bonded to platinum,[25] therefore also confirming the presence of a carbonyl ligand at the platinum center in each isomer.

Thus, the low-temperature ^{31}P and ^{195}Pt NMR spectra clearly point toward a common metal framework from which the geometrical isomers **1a**−**c** are derived. The platinum center is square planar[4b] and 16 electron, while each osmium center adopts the expected 18 electron *pseudo*-octahedral geometry. The equatorial placement of the phosphine ligands about the trinuclear metal framework is in accord with the normal trend observed for trinuclear clusters of osmium.[26] The migration of a triphenylphosphine group to osmium in exchange for a carbonyl during the formation of the complex is perhaps not unexpected; Stone has reported that this is a common reactivity pattern of $(\eta^2\text{-}C_2H_4)Pt(PPh_3)_2$ with carbonyl-bearing species.[27] Furthermore, a similar result was noted in the reaction of $(\eta^2\text{-}C_2H_4)Pt(PPh_3)_2$ with $Re_2(\mu\text{-}H)_2(CO)_8$. Interestingly in this case, the intermediate complex, with both phos-

(22) Verkade, J. G.; Quin, L. D. *^{31}P NMR in Stereochemical Analysis*; VCH: Deerfield Beach, FL, 1987; Chapters 6, 13, and 14.

(23) Pregosin, P. S.; Kunz, R. W. *^{31}P and ^{13}C NMR of Transition Metal Complexes*; NMR Basic Principles and Progress 16; Diehl, P., Fluck, E., Kosfeld, R., Eds.; Springer-Verlag: New York, 1979.

(24) For example, significant steric repulsion between *syn*-phosphites is reported in $Os_3(CO)_6[P(OMe)_3]_6$ (Alex, R. F.; Einstein, F. W. B.; Jones, R. H.; Pomeroy, R. K. *Inorg. Chem.* **1987**, *26*, 3175).

(25) Mann, B. E.; Taylor, B. F. *^{13}C NMR Data for Organometallic Compounds*; Academic: New York, 1981; p 181.

(26) (a) Alex, R. F.; Pomeroy, R. K. *Organometallics* **1987**, *6*, 2437. (b) Deeming, A. J. *Adv. Organomet. Chem.* **1986**, *26*, 1 and references therein.

(27) Farrugia, L. J.; Howard, J. A. K.; Mitrprachachon, P.; Stone, F. G. A.; Woodward, P. *J. Chem. Soc., Dalton Trans.* **1981**, 1274.

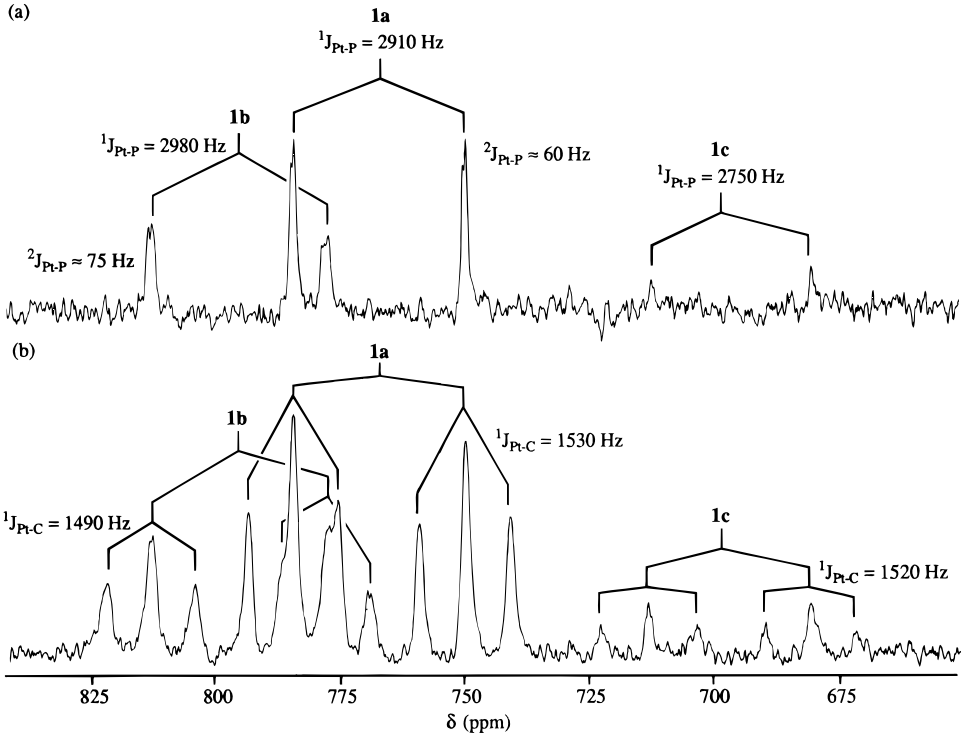

Figure 2. ^{195}Pt NMR spectra of **1** at −70 °C in CD_2Cl_2 with (a) natural abundance ^{13}CO and (b) ≥50% ^{13}CO enrichment.

phines still on platinum, was observed also.[28] The latter undergoes irreversible CO/PPh_3 exchange between Re and Pt to give a mixture of two isomers of $Re_2Pt(\mu\text{-}H)_2(CO)_8(PPh_3)_2$. Contrary to **1a**, the major isomer has the PPh_3 ligand on Re perpendicular to the trimetallic framework.[21,28]

X-ray Crystal Structure of 1a. To gain further confirmation of the molecular geometry of compound **1** and to obtain precise metrical parameters, a single-crystal X-ray analysis was performed. Unfortunately, the small size and poor quality of the crystals, coupled with pseudosymmetry disorder, led to a poorly refined structure (see Experimental Section). Nonetheless, the basic structural features of the cluster are clear (Figure 3). As deduced from the spectroscopic data, the platinum center is square planar and bears one triphenylphosphine and one carbonyl ligand, while the osmium centers are distorted octahedrons. One osmium supports four terminal carbonyl ligands; the other is bonded to one triphenylphosphine and three carbonyl ligands. In particular, the phosphine ligands are disposed in a roughly linear arrangement along the extensions of an osmium−platinum bond, thus confirming the anticipated geometry for the major isomer **1a**. As noted previously, the equatorial placement of the PPh_3 ligands is in accord with the normal trend for trinuclear osmium complexes.[26] The axial orientation of the PPh_3 ligand in the major isomer of $Re_2Pt(\mu\text{-}H)_2(CO)_8(PPh_3)_2$[21] is probably due to the greater steric restraints imposed by the presence of the two bridging hydride ligands in the equatorial plane of this complex.

The Pt−Os(1) and Pt−Os(2) bond lengths are essentially equal, 2.691(3) and 2.680(4) Å, respectively and are similar to the Pt−Os bond lengths in the parent compound $Os_2Pt(CO)_{10}$ (2.689(1) and 2.678(1) Å).[2c] The Os(1)−Os(2) distance of 2.916(4) Å is slightly longer

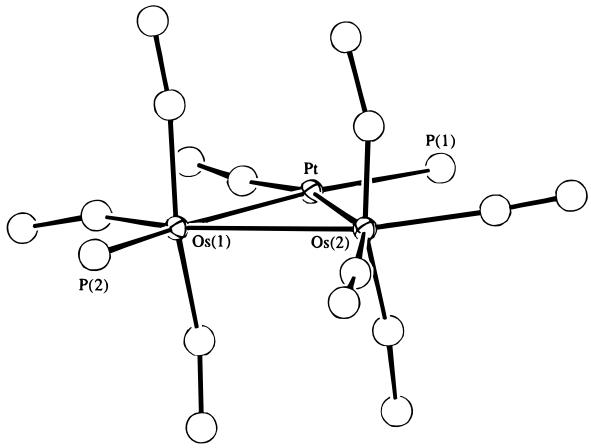

Figure 3. ORTEP drawing of **1a** with relevant atom numbering. The phenyl groups on phosphorus have been omitted for clarity. Selected bond distances (Å): Pt−Os(1) 2.691(3), Pt−Os(2) 2.680(4), Os(1)−Os(2) 2.916(4), Pt−P(1) 2.40(2), Os(1)−P(2) 2.34(2). The P(1)−Pt−Os(1)−P(2) torsion angle is 27.4°.

than that in $Os_2(CO)_8(\mu\text{-}\eta^1,\eta^1\text{-}C_2H_4)$ (2.883(1) Å),[29] $Os_3(CO)_{12}$ (2.887(3) Å),[30] and $Os_2Pt(CO)_{10}$ (2.864(1) Å).[2c]

Isomer Interconversion. The temperature dependence of the ^{31}P NMR spectra clearly suggests that the three distinct isomers observed at −70 °C are interconverting at +95 °C to give an averaged spectrum. Since the line shape changes with temperature are reversible, and the spin−spin couplings are maintained at all temperatures, the isomer interconversion must be intramolecular. At −20 °C, the resonances of isomers **1a** and **1c** are much broader than that of **1b**. This indicates that exchange between isomers **1a** and **1c** is occurring at this temperature, as yet without significant

(28) Beringhelli, T.; D'Alfonso, G.; Minoja, A. P. *Organometallics* **1991**, *10*, 394.

(29) Motyl, K. M.; Norton, J. R.; Schauer, C. K.; Anderson, O. P. *J. Am. Chem. Soc.* **1982**, *104*, 7325.

(30) Churchill, M. R.; De Boer, B. G. *Inorg. Chem.* **1977**, *16*, 878.

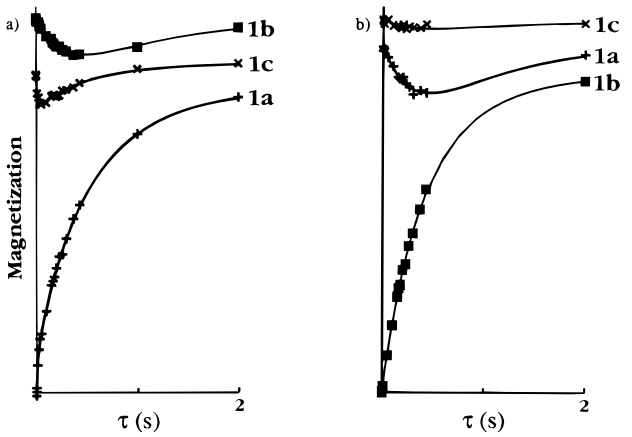

Figure 4. Plots showing the evolution of magnetization vs delay time (τ) of the spin inversion magnetization transfer experiments in the ^{31}P NMR at −50.5(5) °C: (a) results from selective inversion of the signal belonging to isomer **1a**; (b) results from selective inversion of the signal belonging to isomer **1b**.

involvement of **1b**. However, the **1b** resonance broadens at 0 °C and all three signals coalesce near +20 °C; this, coupled with the narrowing to an average spectrum at +95 °C, indicates that isomer **1b** must also be exchanging with isomer **1a** and/or isomer **1c**. Line shape simulations based on the exchange pathways

$$\begin{array}{l} \mathbf{1a} \underset{k_{-1}}{\overset{k_1}{\rightleftharpoons}} \mathbf{1b} \\ \mathbf{1a} \underset{k_{-2}}{\overset{k_2}{\rightleftharpoons}} \mathbf{1c} \end{array} \qquad (4)$$

gave reasonable agreement between calculated and observed spectra, but the precision of the rate constants obtained was low.

In order to delineate the nature of the exchange pathways more precisely, ^{31}P NMR selective inversion magnetization transfer experiments[31] were undertaken. The data obtained for the experiments at −50.5(5) °C are given in Figure 4. Qualitatively, these results confirm the proposed mechanism of exchange. Inversion of the signal belonging to **1a** is followed by initial rapid decreases in the intensities of the signals for **1b** and **1c** due to direct exchange between **1a** and these isomers, while selective inversion of the signal belonging to **1b** results in an initial rapid decrease in the intensity of the signal for isomer **1a** only, followed by a later decrease in the **1c** signal due to the two-step **1b** → **1a** → **1c** magnetization transfer pathway. The magnitudes of the initial slopes of the magnetization *vs* time curves in Figure 4 indicate the relative magnitudes of the corresponding exchange rate constants and show clearly that the rate of the **1a** → **1c** transfers is about 15 times that for the **1a** → **1b** transfers at −50.5(5) °C. The selective inversion magnetization transfer results do not exclude the possibility of direct **1b** → **1c** exchange, only that the rate of direct transfer is far slower than the rate of the indirect **1b** → **1a** → **1c** process over the temperature range studied. The magnetization transfer results afford accurate determination of the activation parameters for the two exchange processes (see Experimental Section) and give $\Delta G^{\ddagger}_{215} = 11.8(4)$ kcal·mol^{-1} for **1a** ⇄ **1c** and 13.0(4) kcal·mol^{-1} for **1a** ⇄ **1b** isomerizations.

On the basis of the isolobal relation[16]

$$(OC)_4Os{=}Os(CO)_3PPh_3 \leftrightarrow H_2C{=}CHR$$

the exchange between isomers **1a** and **1b** can be likened to the well-known rotation of an olefin at a transition metal center, *i.e.* rotation of the diosmium fragment about an axis extending from the $Pt(CO)PPh_3$ moiety, Scheme 1a. The thesis that the isomerization occurs as a result of the flexibility of the trinuclear metal core has precedence in the literature.[32−34] Rotation of the homobimetallic portion of the trinuclear clusters $MRh_2(\mu\text{-}CO)_2(CO)_5(\eta^5\text{-}C_5Me_5)_2$ (M = Mo, W) was initially proposed as one explanation for their variable-temperature ^{13}C NMR features.[33a] The synthesis of the unsymmetric analog $MoCoRh(\mu\text{-}CO)_2(CO)_5(\eta^5\text{-}C_5Me_5)_2$ confirmed this proposal; rotation of the $CoRh(\mu\text{-}CO)_2(C_5Me_5)_2$ fragment about the $Mo(CO)_5$ group was directly observed by variable-temperature ^{13}C NMR spectroscopy.[33b] A similar motion has been proposed to account for the fluxional behavior of $Os_2Cr(CO)_{11}[P(OMe)_3]_2$.[34] In this case, the $Os_2(CO)_6[P(OMe)_3]_2$ group rotates about the $Cr(CO)_5$ unit. Further, Stone has described in detail the analogy of the rotation of a bimetallic fragment, within a triangular metal framework, to that of an olefin rotating about an ML_n fragment.[32]

The free energy of activation of 13.0(4) kcal·mol^{-1} at 215 K for the **1a**/**1b** exchange can be compared with that of $\Delta G^{\ddagger}_{258} = 12.5(3)$ kcal·mol^{-1} in $MoCoRh(\mu\text{-}CO)_2(CO)_5(\eta^5\text{-}C_5Me_5)_2$.[33b] It is interesting that, in the isolobal $PtRh_2(\mu\text{-}CO)_2(CO)(PPh_3)(\eta^5\text{-}C_5Me_5)_2$, rotation of the dirhodium fragment is not observed.[35] In this case, however, the interaction of the μ-CO ligands with the square-planar platinum center acts to anchor the Rh_2 portion of the molecule and inhibits its rotation.[32] Since no such interactions are present in complex **1**, the diosmium fragment is presumably free to rotate about the platinum center without much hindrance.

Interconversion of **1a** and **1c** can be envisaged to proceed *via* two possible mechanisms. As the **1a**/**1b** isomerization, exchange of **1a** and **1c** could involve a rotation of the $(OC)_4Os{=}Pt(CO)PPh_3$ fragment about the $Os(CO)_3PPh_3$ moiety, Scheme 1c. On the other hand, the **1a**/**1c** interconversion could also occur *via* a restricted trigonal twist[26a] at the phosphine-substituted osmium center, Scheme 1b. As detailed in the scheme, if the latter mechanism were operative, the restricted trigonal twist at the phosphine-substituted osmium center would result in exchange of an axial carbonyl of **1a** with an equatorial carbonyl of **1c** (*1* ⇄ *18*), and exchange of an equatorial carbonyl in **1a** with the axial carbonyls in **1c** (*6* ⇄ *13*). Clearly, in order to probe this possibility, complete assignment and a clear understanding of the variable-temperature features of the ^{13}C NMR spectra were required.

(31) Muhandiram, D. R.; McClung, R. E. D. *J. Magn. Reson.* **1987**, *71*, 187.

(32) Barr, R. D.; Green, M.; Howard, J. A. K.; Marder, T. B.; Orpen, A. G.; Stone, F. G. A. *J. Chem. Soc., Dalton Trans.* **1984**, 2757.

(33) (a) Barr, R. D.; Green, M.; Marsden, K.; Stone, F. G. A.; Woodward, P. *J. Chem. Soc., Dalton Trans.* **1983**, 507. (b) Barr, R. D.; Green, M.; Howard, J. A. K.; Marder, T. B.; Stone, F. G. A. *J. Chem. Soc., Chem. Commun.* **1983**, 759.

(34) Davis, H. B.; Einstein, F. W. B.; Johnston, V. J.; Pomeroy, R. K. *J. Am. Chem. Soc.* **1988**, *110*, 4451.

(35) Green, M.; Mills, R. M.; Pain, G. N.; Stone, F. G. A.; Woodward, P. *J. Chem. Soc., Dalton Trans.* **1982**, 1309.

Scheme 1. Possible Mechanisms for Isomer Rearrangement in Compound 1

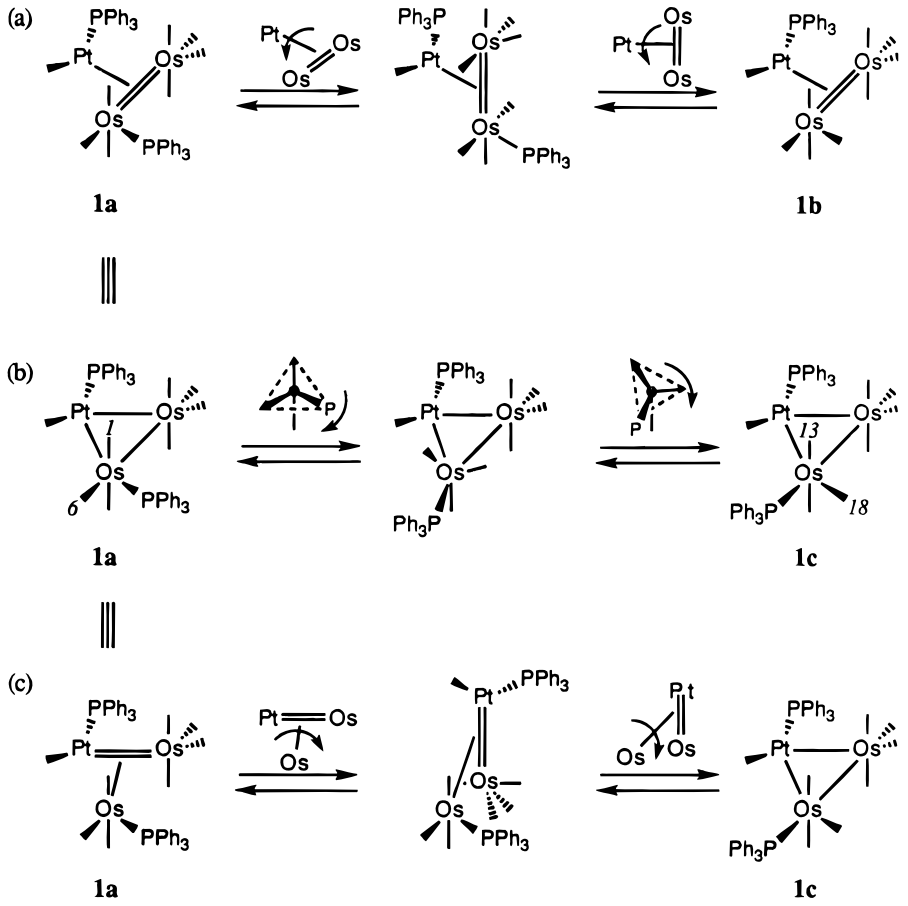

Variable-Temperature ^{13}C NMR Spectroscopic Studies. The −70 °C spectrum (Figure 5) is understandably complex, but reliable integration of the resonances allowed the identification of the signals belonging to each of the three isomers. Within each set, six resonances are observed in a 2:2:1:1:0.66:1 ratio for the two pairs of axial carbonyls and the four inequivalent equatorial carbonyls; the axial carbonyls at each osmium center are rendered equivalent by the mirror plane through the three metals, but the two pairs are themselves inequivalent. The three signals of relative integration 0.66 (*3*, **1a**; *9*, **1b**; *15*, **1c**) are due to the platinum-bonded carbonyl. The relative integration of 0.66 for the main peaks results from the 33.8% natural abundance of ^{195}Pt which causes platinum satellites, each with relative integration 0.17, to flank the main signal. The $^{1}J_{Pt-C}$ coupling constants match those observed in the ^{195}Pt NMR spectrum of Figure 2 ($^{1}J_{Pt-C}$ = 1540 (**1a**), 1490 (**1b**), 1540 Hz (**1c**)). The overlap of the platinum satellites of **1a** and **1c** at δ 185.3 and those of **1a**−**c** at δ 170.0 is due to the accidental superposition of signals *3* and *15*, the similar chemical shift of resonance *9*, and the similar magnitude of the $^{1}J_{Pt-C}$ coupling constants.

Within each isomer, the lowest field carbonyl signal of intensity two (*1*, **1a**; *7*, **1b**; *13*, **1c**) is assigned to the axial carbonyl ligands at the phosphine-substituted osmium center. This is in accord with well-established trends that substitution by a σ-donor ligand causes downfield shift of the ^{13}CO resonance.[26] The upfield carbonyl singlets of intensity two (*2*, **1a**; *8*, **1b**; *14*, **1c**) are thus assigned to the axial carbonyls at the unsubstituted osmium centers. The fact that the axial carbonyl signals are found downfield of the equatorial carbonyl signals in each isomer is also consistent with the normal trend in trinuclear clusters of osmium.[26]

The assignment of the remaining three osmium-bonded equatorial carbonyl ligands in each isomer was aided by the observation of $^{3}J_{P-C}$ coupling for the carbonyls *trans* to a triphenylphosphine ligand across an Os−Pt bond. For instance, in isomer **1b**, the resonance for carbonyl *9*, which is unequivocally assigned to the carbonyl ligand attached to platinum, is split into a doublet ($^{3}J_{P-C}$ = 20 Hz). It is noteworthy that no such coupling was observed through homonuclear Os−Os bonds in phosphine-/phosphite-substituted triosmium carbonyl clusters.[26]

Following this line of reasoning, the signal due to carbonyl *11*, the one *trans* to P_c, is also expected to be a doublet. Its doublet appearance ($^{3}J_{P-C}$ = 14 Hz) is evident at −50 °C but is obscured by overlap with carbonyl *5* at −70 °C. That the doublets are due to three-bond phosphorus-carbon coupling is further corroborated by the fact that, at −70 °C, the ^{31}P NMR spectrum of the ^{13}CO-enriched sample shows ^{13}C satellites for both signals of isomer **1b** ($^{3}J_{P-C}$ = 22 Hz for P_d and $^{3}J_{P-C}$ = 14 Hz for P_c). The remaining carbonyls of isomer **1b**, *10* and *12*, are widely separated and are confidently assigned on the basis of the trend of downfield shift of the carbonyl resonance with phosphine substitution.[26] Accordingly, carbonyl *10* is assigned to the upfield signal at δ 172.6 and carbonyl *12* to the downfield signal at δ 181.1.

In isomer **1c**, the signal at δ 181.7 is a doublet ($^{3}J_{P-C}$ = 15 Hz) and consequently is attributed to carbonyl *18*. It should be noted also that this is the farthest downfield

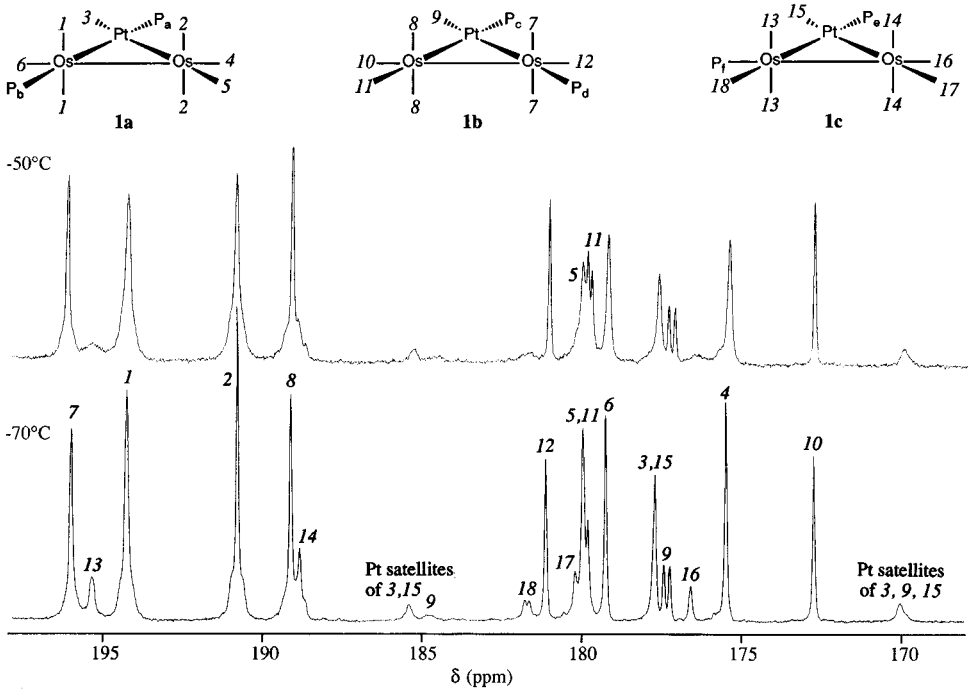

Figure 5. Variable-temperature ^{13}C NMR spectra of **1** at 100.6 MHz in CD_2Cl_2.

equatorial carbonyl signal in isomer **1c**, which is in accord with its attachment to the triphenylphosphine-substituted osmium center, and thus further corroborates the structural assignment of the isomer. The signals due to carbonyls *16* and *17* were identified by analogy to those assigned more rigorously in **1b**; that is, the higher field signal of the two is assigned to carbonyl *16*, the one along the extension of the homonuclear Os−Os bond.

For the signals of isomer **1a**, there are no distinct NMR features, such as doublets due to phosphorus splitting, to aid in the structural assignment of the equatorial carbonyls. Carbonyl *4*, on the extension of the Os−Os bond, can be confidently assigned to the furthest upfield signal at δ 175.4 on the basis of the assignments established for isomer **1b**. However, unequivocal assignment of the signals at δ 180.2 and 179.2 to equatorial carbonyls *5* and *6* is not possible on the basis of chemical shift arguments alone.

Delineation of the **1a**/**1c** exchange process presents an opportunity for both determining the assignment of the *5*/*6* carbonyls of isomer **1a** and for establishing the mechanism of the **1a**/**1c** isomerization. As mentioned before, a restricted trigonal twist at the phosphine-substituted osmium center would result in exchange of axial carbonyls *1* in **1a** with equatorial carbonyl *18* of **1c** and exchange of the equatorial carbonyl *6* in **1a** with axial carbonyls *13* in **1c**, Scheme 1b. In effect, the process will lead to exchange between all carbonyls bonded to the phosphine-substituted osmium centers of isomers **1a**,**c** (*1*, *6*; *13*, *18*). On the other hand, if the isomerization was to occur by a metal-olefin rotation as in Scheme 1c, there would be no exchange of the axial and equatorial sites; instead, equatorial carbonyls *6* and *18*, and axial carbonyls *1* and *13*, would be exchanging. In either case, equatorial carbonyl *6* of isomer **1a** could be positively assigned either to the signal at δ 180.2 or 179.2 on the basis of the observed exchange behavior.

To unambiguously identify the exchange related to carbonyl sites, ^{13}C NMR spin saturation transfer experiments[36] were carried out at −60 °C. Irradiation of the axial carbonyl resonance *1* of **1a**, at δ 194.2, was accompanied by a decrease in intensity of the equatorial carbonyl signal *18* of **1c**; corresponding intensity decreases were also observed in the axial carbonyls *13* of **1c** and the equatorial carbonyl of isomer **1a** at δ 179.2. A small decrease in intensity at axial site *7* of isomer **1b** was also present and is consistent with the known slow exchange between isomers **1a** and **1b**. Irradiation of the equatorial signal at δ 179.2 (**1a**) resulted in a loss of intensity in the axial carbonyl site *13* of isomer **1c** with concomitant intensity decreases at sites *1* (**1a**) and *18* (**1c**). Clearly, these results implicate a restricted trigonal twist rotation at the phosphine-substituted osmium center as being responsible for the **1a** ⇄ **1c** exchange process. Finally, we are also in a position to complete the assignment of the carbonyl signals in isomer **1a**; the resonance at δ 179.2 is due to the exchanging carbonyl *6*, and the sole remaining carbonyl *5* is assigned to the signal at δ 180.2.

The action of a restricted trigonal twist mechanism in **1** at such low temperature was unexpected, since similar processes in phosphine-/phosphite-substituted trinuclear osmium clusters typically occur at higher temperature.[26] For instance, the rates in $Os_3(CO)_{10}[P(OMe)_3]_2$ and $Os_3(CO)_9[P(OMe)_3]_3$ are 31(1) s^{-1} at +17 °C and 40(2) s^{-1} at −2 °C, respectively.[26a] The corresponding rate in **1** is already 11.7(9) s^{-1} at −50 °C. Also, isomer interconversion by the same mechanism in $Os_2Rh(CO)_8(\eta^5\text{-}C_5H_5)PMe_3$ was reported to occur only above −20 °C and a comparable rate constant of 18(1) s^{-1} was observed only at +10 °C.[19]

The greater facility of this process in **1** is reflected by the free energy of activation of 11.8(4) kcal·mol^{-1} at 215 K when compared with $\Delta G^{\ddagger}_{303} = 15.1(4)$ kcal·mol^{-1} for $Os_2Rh(CO)_8(\eta^5\text{-}C_5H_5)PMe_3$,[19] $\Delta G^{\ddagger}_{290} = 15.0(4)$ kcal·mol^{-1} for $Os_3(CO)_{10}[P(OMe)_3]_2$, and $\Delta G^{\ddagger}_{271} = 13.8(4)$ kcal·mol^{-1}

(36) Sandström, J. *Dynamic NMR Spectroscopy;* Academic Press: London, 1982; p 53.

for $Os_3(CO)_9[P(OMe)_3]_3$.[26a] Interestingly, a comparably low value of 10.6(4) kcal·mol^{-1} at 228 K was found for the trigonal twist process which brings about isomer interconversion in $Os_3(CO)_8[P(OMe)_3]_4$.[26a] The source of the steady decrease in activation energy in the $Os_3(CO)_{12-x}[P(OMe)_3]_x$ ($x = 2, 3, 4$) series was attributed to the activating effect of the phosphite ligands through electron donation. However, it is not immediately apparent why the restricted trigonal twist mechanism in **1** is so facile.[37]

Conclusions

Octacarbonyldiosmacyclobutane, $Os_2(CO)_8(\mu\text{-}\eta^1,\eta^1\text{-}C_2H_4)$, reacts readily with $(\eta^2\text{-}C_2H_4)Pt(PPh_3)_2$ to generate the *triangulo*-heterotrinuclear cluster $Os_2Pt(CO)_8(PPh_3)_2$ (**1**) and, as such, may prove to be a useful synthon in the production of metal frameworks of greater complexity.

In solution, compound **1** exists as a system of three interconverting isomers which were characterized by a combination of ^{13}C, ^{31}P, and ^{195}Pt NMR spectroscopies. Of particular spectroscopic interest was the observation of $^3J_{P-C}$ coupling when the triphenylphosphine and carbonyl ligands were disposed in a *trans* arrangement along the extensions of an osmium−platinum bond. This type of long-range coupling between a carbonyl and phosphine is not commonly observed.

Magnetization transfer experiments were conducted at low temperature to establish the mechanisms and energetics of the isomerization processes. One pathway involved a low-energy restricted trigonal twist motion at the phosphine-substituted osmium center of isomers **1a** and **1c**. Of greater interest was the **1a**/**1b** isomerization which occurred *via* a rearrangement of the flexible triangular metal framework and involved rotation of the diosmium fragment, in a metal−olefin fashion, about an axis extending from the platinum center.

Experimental Section

General Procedures. All manipulations were performed under a static atmosphere of purified nitrogen or argon using standard Schlenk techniques. Solvents were dried by refluxing under nitrogen with the appropriate drying agent and were distilled just prior to use. CD_2Cl_2 was dried over P_2O_5 and vacuum distilled, while $CDCl_3$ and toluene-d_8 were dried over molecular sieves prior to NMR sample preparation. $Os_2(CO)_8(\mu\text{-}\eta^1,\eta^1\text{-}C_2H_4)$,[10] ^{13}CO-enriched $Os_2(CO)_8(\mu\text{-}\eta^1,\eta^1\text{-}C_2H_4)$,[18] and $(\eta^2\text{-}C_2H_4)Pt(PPh_3)_2$[20] were prepared by published procedures.

Infrared spectra were recorded on a Bomem MB-100 FT-IR spectrometer, and NMR spectra were obtained on Bruker WM-360 (^1H) and AM-400 (^{13}C, ^{31}P, ^{195}Pt) spectrometers. ^1H and ^{13}C NMR chemical shifts (δ) were internally referenced to solvent and are reported in ppm relative to tetramethylsilane (TMS), while ^{31}P NMR chemical shifts were externally referenced to 85% H_3PO_4. ^{195}Pt NMR chemical shifts are reported relative to $\delta = 0.0$ ppm at the standard frequency of 21.4 MHz as related to the proton resonance of TMS at a frequency of 100 MHz exactly.[38] For the present samples, spectrometer, and solvent, this corresponds to 86.629 MHz. The NMR sample tubes were flame-sealed under vacuum. Fast atom bombardment mass spectra (FAB-MS) were recorded on an AEI-MS9 mass spectrometer with positive xenon ionization (+FAB). Elemental analyses were performed by the Microanalytical Laboratory of this department.

Reaction of $Os_2(CO)_8(\mu\text{-}C_2H_4)$ with $(\eta^2\text{-}C_2H_4)Pt(PPh_3)_2$. $Os_2(CO)_8(\mu\text{-}C_2H_4)$ (62.4 mg, 0.0987 mmol) and 15 mL of benzene were placed in a 3-necked 100 mL flask, and 15 mL of a 5.0 mg/mL benzene solution of $(\eta^2\text{-}C_2H_4)Pt(PPh_3)_2$ (75 mg, 0.100 mmol) was added to the stirred $Os_2(CO)_8(\mu\text{-}C_2H_4)$ solution *via* a cannula at room temperature. An immediate color change from pale yellow to orange was observed. The solution was stirred overnight (*ca.* 16 h) and the solvent was removed *in vacuo*, leaving an orange residue. The residue was extracted with 3 × 1 mL of CH_2Cl_2 and was loaded, under argon, onto a 20 × 4 cm silica-gel column packed in hexane. The column was eluted with 5:1 hexane/CH_2Cl_2. Two mobile bands (yellow and orange) separated cleanly. The solvent was removed *in vacuo* from each fraction. The yellow residue was crystallized from pentane at −80 °C to yield a yellow powder of uncertain composition (5.3 mg) (see below for explanation), and the residue from the orange band was crystallized from CH_2Cl_2/pentane to give $Os_2Pt(CO)_8(PPh_3)_2$ (**1**) as an orange powder (95.2 mg, 73%). An analytically pure sample was obtained by recrystallizing the orange powder from diethyl ether/pentane. Anal. Calcd for $C_{44}H_{30}O_8P_2PtOs_2$: C, 39.91; H, 2.28. Found: C, 40.04; H, 2.16. IR: (pentane, ν_{CO}) 2074 w, 2031 s, 2025 sh, 2012 w, 1989 s, 1983 s, 1967 m, 1956 w, 1948 sh, 1942 sh, cm^{-1}; (CH_2Cl_2, ν_{CO}) 2072 w, 2025 s, 2008 sh, 1984 s, 1964 sh, 1951 sh, 1939 sh, cm^{-1}. ^1H NMR (360 MHz, $CDCl_3$): δ 7.4−7.5 (m, $P(C_6H_5)_3$). $^{31}P\{H\}$ NMR (162 MHz): CD_2Cl_2, −70 °C, δ 22.18 (d, $^3J_{P-P} = 49$ Hz, with Pt satellites, $^1J_{Pt-P} = 2913$ Hz, Pt−P, **1a**), 19.54 (d, $^3J_{P-P} = 2$ Hz, with Pt satellites, $^1J_{Pt-P} = 2990$ Hz, Pt−P, **1b**), 19.00 (d, $^3J_{P-P} = 5$ Hz, with Pt satellites, $^1J_{Pt-P} = 2756$ Hz, Pt−P, **1c**), 3.29 (d, $^3J_{P-P} = 2$ Hz, with Pt satellites, $^2J_{Pt-P} = 85$ Hz, Os−P, **1b**), 3.19 (d, $^3J_{P-P} = 49$ Hz, with Pt satellites, $^2J_{Pt-P} = 60$ Hz, Os−P, **1a**), 2.48 (d, $^3J_{P-P} = 5$ Hz, with Pt satellites, $^2J_{Pt-P} = 25$ Hz, Os−P, **1c**), **1a**:**1b**:**1c** = 4.7:3.4:1.0; toluene-d_8, +95 °C, δ 20.02 (d, $^3J_{P-P} = 30$ Hz, with Pt satellites, $^1J_{Pt-P} = 2930$ Hz, Pt−P), 3.50 (d, $^3J_{P-P} = 30$ Hz, with Pt satellites, $^2J_{Pt-P} = 48$ Hz, Os−P). ^{195}Pt NMR (85.6 MHz, CD_2Cl_2, −70 °C): δ 794.7 (dd, $^1J_{Pt-P} = 2980$ Hz, $^2J_{Pt-P} = 75$ Hz, **1b**), 766.3 (dd, $^1J_{Pt-P} = 2910$ Hz, $^2J_{Pt-P} = 60$ Hz, **1a**), 696.5 (d, $^1J_{Pt-P} = 2750$ Hz, **1c**); ^{13}CO enriched (≥50%), δ 794.7 (d, $^1J_{Pt-P} = 3000$ Hz, with ^{13}C satellites, $^1J_{Pt-C} = 1490$ Hz, **1b**), 766.3 (d, $^1J_{Pt-P} = 2910$ Hz, with ^{13}C satellites, $^1J_{Pt-C} = 1530$ Hz, **1a**), 696.5 (d, $^1J_{Pt-P} = 2770$ Hz, with ^{13}C satellites, $^1J_{Pt-C} = 1520$ Hz, **1c**). ^{13}C NMR (100.6 MHz, CD_2Cl_2, CO region only): −70 °C, δ 195.9 (s, 2C, **1b**), 195.3 (s, 2C, **1c**), 194.2 (s, 2C, **1a**), 190.7 (s, 2C, **1a**), 189.0 (s, 2C, **1b**), 188.8 (s, 2C, **1c**), 181.7 (d, $^3J_{P-C} = 15$ Hz, 1C, **1c**), 181.1 (s, 1C, **1b**), 180.5 (s, 1C, **1c**), 180.2 (s, 1C, **1a**), 180.1 (d, $^3J_{P-C} = 14$ Hz, 1C, **1b**),[39] 179.2 (s, 1C, **1a**), 177.7 (s, with Pt satellites, $^1J_{Pt-C} = 1540$ Hz, Pt−C, **1a** + **1c**), 177.3 (d, $^3J_{P-C} = 20$ Hz, with Pt satellites, $^1J_{Pt-C} = 1490$ Hz, Pt−C, **1b**), 176.5 (s, 1C, **1c**), 175.4 (s, 1C, **1a**), 172.7 (s, 1C, **1b**). $^{31}P\{H\}$ NMR on a ^{13}CO-enriched (≥50%) sample (162 MHz, CD_2Cl_2, −70 °C): δ 22.18 (d, $^3J_{P-P} = 49$ Hz, with Pt satellites, $^1J_{Pt-P} = 2913$ Hz, Pt−P, **1a**), 19.54 (d, $^3J_{P-P} = 2$ Hz, with Pt satellites, $^1J_{Pt-P} = 2984$ Hz, with ^{13}C satellites, $^3J_{P-C} = 14$ Hz, Pt−P, **1b**), 19.00 (d, $^3J_{P-P} = 5$ Hz, with Pt satellites, $^1J_{Pt-P} = 2748$ Hz, with ^{13}C satellites, $^3J_{P-C} = 15$ Hz, Pt−P, **1c**), 3.29 (d, $^3J_{P-P} = 2$ Hz,

(37) Isomerization of $Re_2Pt(\mu\text{-}H)_2(CO)_8(PPh_3)_2$[28] also occurs by a restricted trigonal twist involving the phosphine ligand, but in this case, the exchange involves a *fac* to *mer* rearrangement of the carbonyl ligands (*i.e.* an axial to equatorial phosphine migration) whereas, in $Os_2Pt(CO)_8(PPh_3)_2$, the carbonyls remain in a *mer* configuration (*i.e.* the phosphines remain equatorial). In $Re_2Pt(\mu\text{-}H)_2(CO)_8(PPh_3)_2$, the activation energy for the isomerization process was determined to be 17.7(4) kcal/mol, which is much larger than that for the **1a** ⇄ **1c** exchange in $Os_2Pt(CO)_8(PPh_3)_2$.

(38) (a) Kidd, R. G.; Goodfellow, R. J. In *NMR and the Periodic Table*; Harris, R. K., Mann, B. E., Eds.; Academic: London, 1978; p 250. (b) Goodfellow, R. J. In *Multinuclear NMR*; Mason, J., Ed.; Plenum: New York, 1987; p 533.

(39) The resonance at δ 180.1 is overlapped with the singlet at δ 180.2 at −70 °C; the doublet feature is ascertained from the −50 °C spectrum where a combination of line broadening and temperature dependance of the chemical shifts has separated the resonances (see Figure 5).

with ^{13}C satellites, $^3J_{P-C} = 22$ Hz, Os−P, **1b**), 3.19 (d, $^3J_{P-P} = 49$ Hz, Os−P, **1a**), 2.48 (d, $^3J_{P-P} = 5$ Hz, Os−P, **1c**). FAB-MS (m/e): $M^+ - nCO$, $n = 0-4$, 6, 8.

The first yellow fraction appears to contain predominantly a species of empirical formula $Os_2Pt(CO)_9PPh_3$ judging from the ^{31}P NMR (δ 22.72 (s, with Pt satellites, $^1J_{Pt-P} = 3019$ Hz, Pt−P)), ^{195}Pt NMR (δ 708.5 (d, $^1J_{Pt-P} = 3010$ Hz); ^{13}CO enriched (≥50%) δ 708.5 (d, $^1J_{Pt-P} = 3040$ Hz, with ^{13}C satellites, $^1J_{Pt-C} = 1500$ Hz)), and ^{13}C NMR in the carbonyl region (−70 °C, δ 187.4 (s, 2C, CO_{ax}), 185.3 (s, 2C, CO_{ax}), 176.6 (s, with Pt satellites, $^1J_{Pt-C} = 1520$ Hz, Pt−CO), 175.4 (3C, overlapped, CO_{eq}), 173.1 (s, 1C, CO_{eq})). In particular, the ^{195}Pt NMR spectrum establishes that the platinum center has both phosphine and carbonyl ligands, while the ^{31}P NMR spectrum indicates the presence of a species with only one type of phosphine ligand. However, due to the small amount of material recovered and the presence of inseparable impurities, an analytically pure sample could not be isolated for complete characterization by mass spectrometry and elemental analysis.

^{31}P NMR Spin Inversion Magnetization Transfer Experiments. Temperatures were monitored by the use of an external Sensotek BAT-10 copper thermocouple inserted into a toluene solution in a 5 mm o.d. NMR tube and are considered accurate to ±0.5 K. The temperature at the probe was allowed to equilibrate for 15 min and was monitored until a steady reading was obtained over a 10 min interval. The temperature was remeasured following the completion of the experiments in order to ascertain any thermal drift. The mean temperature was then used for subsequent calculations.

The selective inversion magnetization transfer experiments were carried out by selectively inverting the ^{31}P NMR resonance for the platinum-bonded phosphorus in either isomer **1a** or isomer **1b** and monitoring the temporal behavior of the ^{31}P magnetizations of the platinum-bonded phosphorus atoms in all three isomers by sampling the longitudinal magnetizations at time τ after the inversion. Selective inversion was accomplished using DANTE,[40] spectra at 15−20 values of τ were collected, and the magnetizations (integrated peak intensities) were determined using a common set of spectral processing parameters for each series of experiments. The set of magnetization data for all values of τ (for a particular inversion and temperature) were analyzed by least squares[31] to obtain the values of the rate constants k_1 and k_2 and estimates of their uncertainties. In order to obtain more reliable estimates of the rate constants, the longitudinal ^{31}P relaxation times (T_1) for each of the platinum-bound phosphorus nuclei were determined by the standard inversion-recovery method[41] at each temperature so that the relaxation parameters in the least-squares iterations could be fixed at the corresponding observed values as suggested by Muhandiram.[31] The equilibrium constants, K_1 and K_2, were obtained from the peak intensities, and simple linear fits of the raw equilibrium constant-temperature data gave improved estimates of the equilibrium constants used in the exchange matrices for the least-squares analysis.[42] The equilibrium constants and the values of the rate constants from the least-squares analyses at their respective temperatures are as follows: 208.4(5) K, $k_1 = 0.14(1)$ s^{-1}, $k_2 = 2.1(2)$ s^{-1}, $K_1 = 0.70(1)$, $K_2 = 0.21(1)$; 213.5(5) K, $k_1 = 0.26(2)$ s^{-1}, $k_2 = 4.0(2)$ s^{-1}, $K_1 = 0.71(1)$, $K_2 = 0.20(1)$; 217.6(5) K, $k_1 = 0.42(2)$ s^{-1}, $k_2 = 6.5(4)$ s^{-1}, $K_1 = 0.71(1)$, $K_2 = 0.18(1)$; 222.7(5) K, $k_1 = 0.74(2)$ s^{-1}, $k_2 = 11.7(9)$ s^{-1}, $K_1 = 0.72(1)$, $K_2 = 0.17(1)$.

The rate constants were fit to the linear form of the Eyring equation by a least-squares linear regression routine. The activation parameters obtained for the two processes were as follows: k_1 (**1a**/**1b** exchange), $\Delta H^\ddagger = 10.1(2)$ kcal·mol^{-1} and $\Delta S^\ddagger = -13.1(11)$ eu; k_2 (**1a**/**1c** exchange), $\Delta H^\ddagger = 10.7(3)$ kcal·mol^{-1} and $\Delta S^\ddagger = -5.2(12)$ eu. The errors reported in the activation parameters are the nonlinear errors[43] as determined from the least-squares regression.

Table 1. Crystal Data and Summary of Intensity Data Collection and Structure Refinement for $Os_2Pt(CO)_8(PPh_3)_2$ (1a)

formula	$C_{44}H_{30}O_8Os_2P_2Pt$
fw	1324.15
cryst syst	orthorhombic
space group	$Pn2_1a$
temp, °C	18
cell constants[a]	
a, Å	16.316(9)
b, Å	14.502(9)
c, Å	17.605(9)
V, Å^3	4165.6
Z	4
D_{calc}, g cm^{-3}	2.11
μ_{calc}, cm^{-1}	101.0
diffractometer/scan	Enraf-Nonius CAD-4/$\omega-2\theta$
range of rel transm factors, %	58/100
radiation, graphite monochromator	Mo Kα ($\lambda = 0.710\ 73$ Å)
max cryst dimens, mm	$0.05 \times 0.18 \times 0.25$
scan width	$0.80 + 0.35 \tan\theta$
std reflcns	800; 0,10,0; 008
decay of stds, %	±1.5
reflcns measd	4102
2θ range, deg	$2 \le 2\theta \le 50$
range of h,k,l	+19,+17,+20
reflcns obs [$F_o \ge 5\sigma(F_o)$][b]	1434
computer programs[c]	SHELX[44]
struct solution	SHELXS[46]
no. of params varied	171
weights	$[\sigma(F_o)^2 + 0.0004F_o^2]^{-1}$
GOF	2.50
$R = \Sigma\|\|F_o\| - \|F_c\|\|/\Sigma\|F_o\|$	0.068
R_w	0.077
R inverse configuration	0.068
largest feature final diff map, e Å^{-3}	0.3

[a] Least-squares refinement of $((\sin\theta)/\lambda)^2$ values for 17 reflections $\theta > 14°$. [b] Corrections: Lorentz−polarization and absorption (empirical, ψ scan). [c] Neutral scattering factors and anomalous dispersion corrections from ref 45.

^{13}C NMR Spin Saturation Transfer Experiments. Conventional double-resonance experiments[36] were employed to selectively irradiate specific resonances in the carbonyl region of the ^{13}C NMR spectrum at −60 °C. Irradiation of the signal at δ 194.2 (CO_{ax}, **1a**) resulted in a 39% decrease in the signal at δ 195.3 (CO_{ax}, **1c**), a 36% loss of intensity in the doublet at δ 181.7 (CO_{eq}, **1c**), a 30% decrease in the signal at δ 179.2 (CO_{eq}, **1a**), and a 6% decrease in the signal at δ 195.9 (CO_{ax}, **1b**). Spin saturation of the signal at δ 179.2 (CO_{eq}, **1a**) resulted in a 32% decrease in the signal at δ 195.3 (CO_{ax}, **1c**), a 27% loss of intensity in the doublet at δ 181.7 (CO_{eq}, **1c**), a 19% decrease in the signal at δ 194.2 (CO_{ax}, **1a**), and a 3% decrease in the signal at δ 195.9 (CO_{ax}, **1b**).

X-ray Crystal Structure Determination of $Os_2Pt(CO)_8(PPh_3)_2$ (1a). An orange single crystal of the title compound was mounted in a thin-walled glass capillary flushed with argon and transferred to the goniometer. The space group was determined to be either the centric $Pnma$ or the acentric $Pn2_1a$ from the systematic absences. The subsequent solution and refinement of the structure was carried out in the acentric space group $Pn2_1a$. A summary of the data collection parameters is given in Table 1.

The available crystals of the compound were small, and the highest observed to measured ratio was only 35%. This,

(40) Morris, G. A.; Freeman, R. *J. Magn. Reson.* **1978**, *29*, 433.
(41) Farrar, T. C.; Becker, E. D. *Pulse and Fourier Transform NMR*; Academic: New York, 1971; pp 20−22.

(42) The exchange matrices for the **1a**/**1b** and **1a**/**1c** exchange processes are as follows:

$$\Pi(\mathbf{1b}/\mathbf{1b}) = \begin{pmatrix} -1 & 1/K_1 & 0 \\ 1 & -1/K_1 & 0 \\ 0 & 0 & 0 \end{pmatrix} \qquad \Pi(\mathbf{1a}/\mathbf{1c}) = \begin{pmatrix} -1 & 0 & 1/K_2 \\ 0 & 0 & 0 \\ 1 & 0 & -1/K_2 \end{pmatrix}$$

(43) Marquardt, D. W.; Bennett, R. G.; Burrell, E. J. *J. Mol. Spectrosc.* **1961**, *7*, 269.

coupled with the pseudosymmetry problem outlined below, resulted in a poorly refined structure. While the gross structural features are quite clear, the overall refinement is poor.

While the space group choice was not unambiguous, the molecule cannot support a mirror plane perpendicular to the Os_2Pt triangle and so the acentric $Pn2_1a$ was attempted first. Pseudomirror correlations became immediately obvious with Os(2) residing on what would be a mirror plane in *Pnma*. Closer examination revealed that if the mirror were present, Pt and Os(1) would be disordered, but only C(3)−O(3) and C(4)−O(4) would not be close to a mirror position. The mirror symmetry is also broken by the staggered nature of the phenyl groups near the Pt−Os(1) axis, but this is not enough to prevent the pseudomirror correlations which play havoc with the refinement.

The current refinement is in $Pn2_1a$. The phenyl groups were refined as rigid groups although the individual thermal parameters were allowed to refine freely. Only the Pt and Os atoms were refined anisotropically. The hydrogen atoms were not included in the final refinement. Refinement as described above led to the final values of $R = 0.068$ and $R_w = 0.077$. The final values of the positional and thermal parameters are given in the Supporting Information.

Acknowledgment. We thank the Natural Sciences and Engineering Research Council of Canada (NSERC) for funding and for an Undergraduate Summer Research Award to J.C. Financial support from University of Alberta is also gratefully acknowledged. The expert assistance of Mrs. G. Aarts and Mr. G. Bigam of the University of Alberta High Field NMR Laboratory in carrying out the ^{31}P NMR spin inversion magnetization transfer and ^{13}C NMR spin saturation transfer experiments is sincerely appreciated. We are also grateful to Dr. John Washington for assistance with the variable-temperature NMR experiments and Dr. Frank Seils for important initial work on this project.

Supporting Information Available: Tables of fractional coordinates with B_e values, thermal parameters, and bond distances and angles and an ORTEP diagram for isomer **1a** (6 pages). Ordering information is given on any current masthead page.

OM950938E

(44) Sheldrick, G. M. SHELX76, a system of computer programs for X-ray structure determination as locally modified, University of Cambridge, England, 1976.
(45) Sheldrick, G. M. SHELXS. *Acta Crystallogr.* **1990**, *A46*, 467.
(46) *International Tables for X-ray Crystallography*; Kynoch: Birmingham, England, 1974; Vol. IV, pp 72, 99, 149.